Eng. & Tech. Journal, Vol.27, No. 8, 2009

Finite Element of Cutting Force in Turning Processes with Differently Coated Tools

Dr. Aseel hamad* **&** **Zena jumaa ***

Received on: 14/4/2008
Accepted on: 5/3/2009

Abstract

The aim of this study is to create a FEM simulation model in order to obtain Numerical solutions of cutting forces, for a range of coated tool materials and defined cutting conditions. Commercial implicit finite element code MSC.Marc has been used in simulations of orthogonal cutting processes performed by means of multi-coated tools. The latter were equipped with progressively increasing number of thin layers including TiC, TiN and Al_2O_3 films deposited onto ISO P20 carbide substrates. Results showing the tool–chip interfacial friction influencing the force distribution fields, as the consequence of using coated tools. The various force simulation results obtained were compared with the measurements of cutting force and discussed in terms of literature data.

This paper also reports the procedure and specific modeling techniques for simulating the orthogonal metal cutting process using a general-purpose finite element computer code. The finding of this paper provides useful insights for understanding and for improving the orthogonal metal cutting process. The predicted value of Fc is in good agrement with the experimentally measured with an error of 8%.

الخلاصة

يهدف البحث الى توليد موديل تحليلي بأستخدام تقنية العناصر المحددة للحصول على قوى القطع لمستوي او لمجموعة من مواد عدد القطع ومعرفة ظروف القطع. البرنامج المستخدم هو (Marc) الذي يستعمل في عمليات القطع العمودي التحليلية للعدد المكسية بمادة كاربيد التيتانيوم(TiC), نتريد التيتانيوم (TiN) واوكسيد الألمنيوم (Al_2O_3) المترسبة على عدة ذو اساس كاربيدي.أظهرت النتائج ان الأحتكاك بين النحاتة والعدة يؤثر على توزيع القوى . وقد تمت مقارنة النتائج مع دراسات سابقة وكان الفارق بينها يصل الى 8% .

1. Introduction

Cutting is one of the most important and common manufacturing processes in industry. Simplified analytical methods have been developed, for example, by Merchant [1] introduced the concept of shear angle and by Lee and Shaffer [2] proposed an analytical model using slip-line field theory. Later, more complicated models [3–5] have been developed which also consider the effects of friction, work-hardening, and temperature. These successful models gave useful insight into the mechanics of cutting.

In recent years, finite element analysis has become the main tool for simulating metal cutting processes.

Early analyses were made by Usui and Shirakashi [6] and Iwata et al. [7] who analyzed the steady-state orthogonal cutting. Chip formation and separation from the work piece was first attempted by Strenkowski and Carroll [8]. Chip formation was achieved by various separation criteria like distance tolerance criterion [9], strain energy density criterion [10, 11], and fracture mechanics based criterion [12]. To deal with large element distortion in metal cutting simulation, Shih and Yang [13] and Shih

* Production Engineering and Metallurgy Department, University of Technology / Baghdad.

https://doi.org/10.30684/etj.27.8.3
2412-0758/University of Technology-Iraq, Baghdad, Iraq

[14, 15] developed a mesh rezoning technique. Ceretti et al. [16] developed a cutting model by deleting elements having reached a critical value of accumulated damage.

It is especially important that FEM analysis can help to investigate some thermodynamical effects occurring in the cutting zone which, as so far, cannot be measured directly. An example for such effects is the influence of cutting tool coatings on the cutting force.

It should be noted that the majority of previous orthogonal metal cutting simulations is devoted to uncoated carbide tools and now the opposite trend to consider single and multiple coatings has been observed. It is estimated [1] that currently about 53% of all cutting tool materials are CVD and PVD coated carbides both in the form of solid tools or indexable inserts. Currently, coatings of different structures containing layers of titanium carbide (TiC), titanium nitride (TiN), titanium carbonitride (Ti(C, N)), aluminum oxide (Al2O3) and titanium aluminum nitride ((Ti, Al)N) are mostly used in metal cutting manufacturing [2,3].

In fact, the first completed work focusing on the evaluation of a predictive orthogonal cutting model for coated carbide tools with multiple coating layers using the FEM was presented by Yen et al.

2. Cutting Force measurements [17]

Forces in machining can be measured in two main ways: directly or indirectly. Direct measurements involve mounting a tool (in turning) or the tool or workpiece (in milling) on a dynamometer, which responds to the forces by creating electrical signals in proportion to them. These measurements are used when the forces need to be known accurately both in magnitude and direction, for example if thrust, feed and the main cutting forces in turning are required as shown in Figure (1), or the torque and thrust force in drilling are needed.

Indirect measurements involve deductions from the machine tool behaviour. For example, the power used by the main spindle motor increases with the main cutting force or torque; and that used by the feed motions can be related to the feed force. Particularly with NC machines, which are fitted with high sensitivity and response main and feed drive motors, indirect methods can be used to determine the active forces. Indirect methods are less accurate than direct methods, but can be sufficient for monitoring purposes. The main consideration here will be direct methods.

Classic orthogonal cutting model for continuous chip formation assumes plane-strain deformation conditions. Basic representation of the process model is illustrated in Fig.2. Geometric relations in orthogonal cutting model yield the following equations for normal and frictional forces, F_n and F_f, on the tool rake face as functions of measured cutting force components, F_c and F_t, and tool rake angle as:

$$F_n=F_c \cos \alpha+F_t \sin \alpha \quad (1)$$

$$F_f=F_c \sin \alpha+F_t \cos \alpha \quad (2)$$

In conventional machining at low cutting speeds, the friction mechanism is mostly effective at the tool flank face.

3. FEA Simulation of Orthogonal Cutting Process

As mentioned the Finite Element model used for the plane-strain orthogonal metal cutting simulation is based on the Lagrangian techniques and explicit dynamic, mechanical modeling software with adaptive remeshing. This means that the initial mesh becomes distorted after a certain length of cut and is remeshed in this vicinity to form a regular mesh again.

In this paper, special attention is focused on the contact zone (friction, heat generation and flow) in order to adapt the desired properties of coating materials to a specific machining task. Basically, cutting tool manufacturers use four major groups of hard coating components. They are: the group of titanium-based materials (TiN, TiC and Ti(C, N)) often supplemented by Al or Cr ((TiAl) N, TiAlON, and CrCN), ceramic coatings like Al_2O_3 and two special groups including super-hard coatings and solid lubricant coatings (MoS_2 or pure graphite WC/C).

3.1 Geometric Modeling

The Finite Element model is composed of a deformable workpiece and a rigid tool. The tool penetrates through the workpiece at a constant cutting speed and variable feed rates. The initial arrangement of both the workpiece and the tool in the simulation model are shown in Figure (3).the length of the workpiece is assumed to be (10 mm); five models are suggested having various cutting conditions as shown in (table 1)

Modeling geometry and dimensions is done using the Cartesian coordinate, 2-D model as shown in Figure (3)

The cutting tool is modeled to be multiple coating as shown in (Figure 4 a, b, c) in order to study in detail the behavior of these layers under different conditions of layers number.

3.2. Mesh Generation

As mentioned previously the Finite Element model used for the plane-strain orthogonal metal cutting simulation is based on the Lagrangian techniques and explicit dynamic, mechanical modeling software with adaptive remeshing. This means that the initial mesh becomes distorted after a certain length of cut. The workpiece discretized by bilinear four-node quadratic.the initial geometry and mesh is presented in Figure(3) which consists of the following number of nodes and elements.

- (669) nodes and (610) elements for uncoated tools models.
- (679) nodes and (619) elements for one coated layer tools models.
- (689) nodes and (628) elements for two coated layer tools models.
- (699) nodes and (637) elements for three coated layer tools models.

The upper part of mesh, which constitutes the removed workpiece material, is finer, to enable the stresses, strains in the chip and tip region to be accurately predicted.

3.3. Load and Boundary Condition

The boundary condition is shown in Figure (5), the left and bottom boundary nodes of the workpiece are fixed in both X and Y directions by gluing them to a rigid curve. Cutting tool is modeled as a rigid and it constrains the vertical displacement [18].

To reduce the effects of boundary conditions, the dimensions of the workpiece are set large enough to maintain steady-state.

Friction is another boundary condition that could have significant consequence to the solution of this metal cutting problem. Due to the difficulty in measuring the friction experimentally, the coefficients of friction between chip and tool is assumed to be constant (μ_p=0.3) for coated tool. [19, 20]

There is one distinct stage of workpiece loading for this problem, namely tool movement toward workpiece. The load cases are executed consecutively in MARC code. The motion of the rigid tools is defined by a prescribed velocity. The position is determined by explicit, forward integration of the velocities based upon the current time step.

3.4 Material Properties

To ensure an accurate FE model, it is necessary that the input material properties are closely matching those of the experimental test workpiece.

The workpiece material used for the plane-strain orthogonal metal cutting simulation is AISI 1045 steel. Its composition and mechanical properties are shown in Tables (2) and (3). Therefore, tensile test specimens were made for the workpiece, by using Instron 1152 servo hydraulic testing machine in the Material Testing Lab of University of Technology. Tool substrate is to be Cemented carbide (WC). Table (4) shows the mechanical properties of (WC); Table (5) shows the mechanical properties of coating layers used in the simulation tests.

3.5 Cutting Tools Inserts

Four types of commercially available tungsten based cemented carbide inserts were tested. The cutting inserts tested were TiN coated – insert 1, TiN/TiC coated – insert 2 and TiN/Al_2O_3/TiC coated – insert 3, respectively. All the inserts were suitable for machining different kinds of steels at high speeds and high feed rates.

All the inserts have identical geometry designated by the American National Standard Institute (ANSI) as [CNMM 120404]. The inserts were rigidly mounted on a right hand style tool holder with a cutting rake and a back rake of –5º. The tool holder is designated by ANSI as [PCLNR 2020 K 12]. [22, 23]
Tool geometry which is used for the orthogonal and experimental test is presented in table (6).

4. Finite Element results

Finite Element simulations of the orthogonal metal cutting process have been carried out for all 15 cases. In each case, the cutting tool is made to advance incrementlly until a steady state is reached. On an average 600-800 displacement increments are required to reach the steady state condition, corresponding to about 4-10 h.

Fig. (6, 7, 8) shows the variation of the horizontal cutting force with the tool tip displacement for three types of tools and one depth, feed rate, velocity value. For each type of tool the cutting force is seen to approach a constant value as the cutting tool advances, indicating the achievement of a stead-state condition. For each tool, the cutting force is seen to increase as the coated layer change, as a result of increased resistance due to friction along the tool-chip interface.

Finite Element simulation results presented below are taken after the cutting tool has moved more than 1.5 mm thus they represent typical steady-state solutions. Because of space limitations, only results for the case of rake angle $\alpha = -5^{\circ}$ are given. Solutions for other rake angles bear similar features.

The cutting force F_c is determined by integrating the stresses acting on both the tool rake face/chip and the flank face/machined interfaces. It can be seen from Fig.(6, 7, 8)That the cutting force increases from zero linearly to a peak value, and then finally gradually approaches steady value. The steady value is the avarage cutting force usually measured in cutting tests. It is apparent that the Finite Element analysis can show more dynamic details of the predicted instantaneous cutting force, while the ordinary cutting tests measure the average cutting forces.

Frome Fig. (9) it can be seen that the tool coated two layers is the smaller value of cutting force reach to (60 N) but tool coated three layers is the larger value reach to (70 N).

It should be pointed out that there might be a difference between the cutting

force and feed force "thrusting" force which is induced by the feed rate Fig.(10 ,11 ,12).The thrusting force heavily depends on the magnitude of the feed rate and workpiece material, and is usually the dominant component in the measured thrust cutting force. On the other hand, in the Finite Element modeling, such a thrusting force is not needed to enforce a feed rate in order to accomplish the cutting process. Therefor, such a thrusting force is not exerted when the boundary conditions were assigned. The lack of this thrusting force would largely reduce the predicted value of thrust force and slightly reduce the predicted cutting force. Frome Fig. (13) it can be seen that the tool coated two layers is the smaller value of feed force reach to (15 N) but tool coated three layers is the larger value reach to (18 N).

5. Conclusions

This study reveals the effects of multi-coated tools model and material data in the simulation of orthogonal cutting.successful finite element simulations of orthogonal metal cutting process have been carried out using the general-purpose finite element code Marc. This was achieved with a judicious combination of a set of advanced modeling options in the code. Dry friction was assumed along the tool-chip interface and was modeled with a modified Coulomb friction law.

A total of 15 simulations have been performed, with cover a range of multi-coated tools. Steady-state finite element solutions for the cutting force have been obtained and representative contour plots for these field quantities have been presented. Several conclusions can be drawn from this stude and from the finite element solutions. First, this study demonstrates that it is possible to carry out sophisticated finite element simulations of metal cutting processes using advanced general-purpose commerical codes. Second, the finite element simulations were able to re-produce experimentally observed phenomena in orthogonal metal cutting. It is believed that details afforded by finite element simulations will greatly benefit the engineer in gaining a better understanding of metal cutting processes and in aiding the design and application of such processes.

References

[1] M.E. Merchant, Mechanics of the metal cutting process, Journal of Applied Physics 16 (1945) 267–318.

[2] E.H. Lee, B.W. Shaffer, The theory of plasticity applied to a problem of machining, ASME Journal of Applied Mechanics 73 (1951) 405–413.

[3] R.G. Fenton, P.L.B. Oxley, Mechanics of orthogonal machining: allowing for the effects of strain-rate and temperature on the tool–chip friction, Proceedings of Institution of Mechanical Engineers 183 (1969) 417–438.

[4] G. Boothroyd, J.A. Bailey, Effects of strain-rate and temperature in orthogonal metal cutting, Journal of Mechanical Engineering Science 8 (1966) 264.

[5] V. Gorianis, S. Kobayashi, Strains and strain-rate distributions in orthogonal metal cutting, Annals of CIRP 15 (1967) 425.

[6] E. Usui, T. Shirakashi, Mechanics of machining from descriptive to predictive theory, on the art of cutting metals, ASME PED 7 (1982) 13–35.

[7] K. Iwata, K. Osakada, Y. Terasaka, Process modeling of orthogonal cutting by the rigid-plastic finite element method, Journal of Engineering Materials and Technology 106 (1984) 132–138.

[8] J.S. Strenkowski, J.T. Carroll, A finite element model of orthogonal metal

cutting, Journal of Engineering for Industry 107 (1985) 347–354.
[9] K. Komvopoulos, S.A. Erpenbeck, Finite element modeling of orthogonal metal cutting, Journal of Engineering for Industry 113 (1991) 253–267.
[10] Z.C. Lin, S.Y. Lin, A coupled finite element model of thermoelastic–
plastic large deformation for orthogonal cutting, Journal of Engineering Material Technology 114 (1992) 218–226
[11] M. Usta, Finite element analysis of orthogonal metal cutting operations, Ph.D. Thesis, Mechanical Engineering Department of Middle East Technical University, Ankara, Turkey, 1999.
[12] J. Hashemi, A.A. Tseng, P.C. Chou, Finite element modeling of continuous and segmental chip formation in high speed orthogonal machining, Journal of Materials Engineering and Performance 3 (6) (1994) 712–721.
[13] A.J. Shih, H.T.Y. Yang, Experimental and finite element predictions of residual stresses due to orthogonal metal cutting, International Journal of Numerical Methods in Engineering 36 (1993) 1487–1507.
[14] A.J. Shih, Finite element analysis of orthogonal metal cutting mechanics, International Journal of Machine Tools Manufacturing 36 (1996) 255–273.
[15] A.J. Shih, Finite element simulation of orthogonal metal cutting, Journal of Engineering for Industry 117 (1995) 84–93.
[16] E. Ceretti, P. Fallbohmer, W.T. Wu, T. Altan, Application of 2D FEM to chip formation in orthogonal cutting, Journal of Materials Processing Technology 59 (1996) 169–180.
[18] Halil Bil, and A. Erman Tekkaya, A Comparison of Orthogonal Cutting Data From Experiments with Three Different Finite Element Models, International Journal of Machine and Manufacture, Vol. 44, pp. 933-944, 2004.
[19] www.guharan.com
[20] www.matweb.com
[21] Halil Bil, and A. Erman Tekkaya, A Comparison of Orthogonal Cutting Data From Experiments with Three Different Finite Element Models, International Journal of Machine and Manufacture, Vol. 44, pp. 933-944, 2004.
[22] Halil Bil, and A. Erman Tekkaya, A Comparison of Orthogonal Cutting Data From Experiments with Three Different Finite Element Models, International Journal of Machine and Manufacture, Vol. 44, pp. 933-944, 2004.
[23] SANDVIK, Main Catalogue, 2006.

Table (1) Cutting Conditions

Material type	AISI 1045
Cutting speed **(V_c)**	125 (m/min.)
Depth of cut **(t)**	0.5, 1, 1.5 ,2 , 2.5 (mm)
Feed rate **(s)**	0.08**,** 0.11, 0.12**,** 0.14, 0.16 (mm/rev.)

Table (2) Nominal Composition AISI 1045 [20].

C%	Si%	Mn%	P%	S%
0.45	0.2	0.58	0.02	0.025

Table (3) Mechanical properties of work material at room temperature [20].

Ultimate stress	(σ_u)	515 Mpa
Yield stress	(σ_y)	484 Mpa
Young's Modulus	(E)	200 Gpa
Poisson´s ratio	(ν)	0.29
Hardness Brinell	HB	170
Shear modulus	(G)	80 Gpa

Table (4) Mechanical properties of Cemented Carbide (WC) cutting tool [20]

Density	(ρ)	14500	kg/m^3
Yield stress	(σ_y)	6000	MPa
Young's Modulus	(E)	650	GPa
Poisson's ratio	(ν)	0.30	

Table (5) Mechanical properties of coating layers [21].

Coating layer	TiC	AL2O3	TiN
Young's Modulus(E)[Gpa]	450-496	340-400	250
Poisson's ratio(n)	0.19-0.24	0.23	0.25
Density(r)**[kg/m$^{3]}$**	4650-49000	3780	4650

Table (6) Tool geometry.

Tool rake angle	-5º
Tool clearance angle	5º
Measured cutting edge radius	40μm

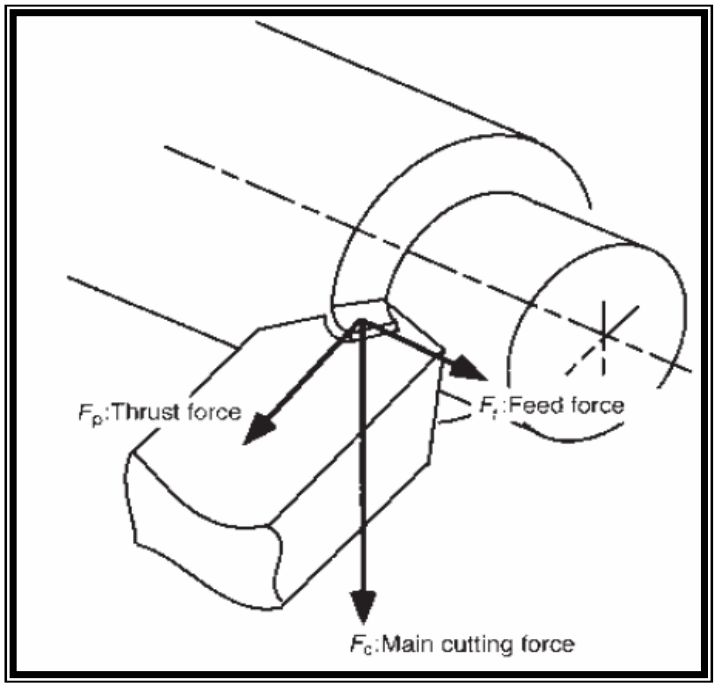

Figure (1) Forces acting on cutting tool in turning

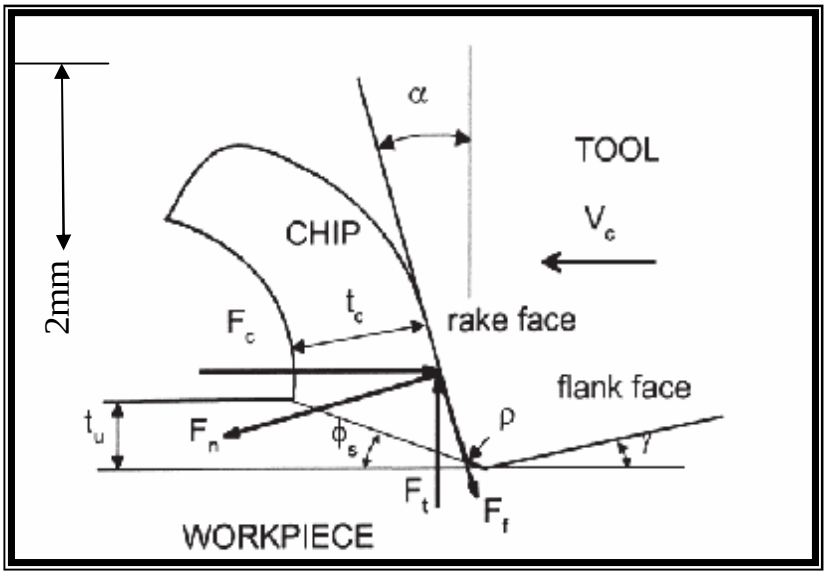

Figure (2) Forces generated during orthogonal cutting process.

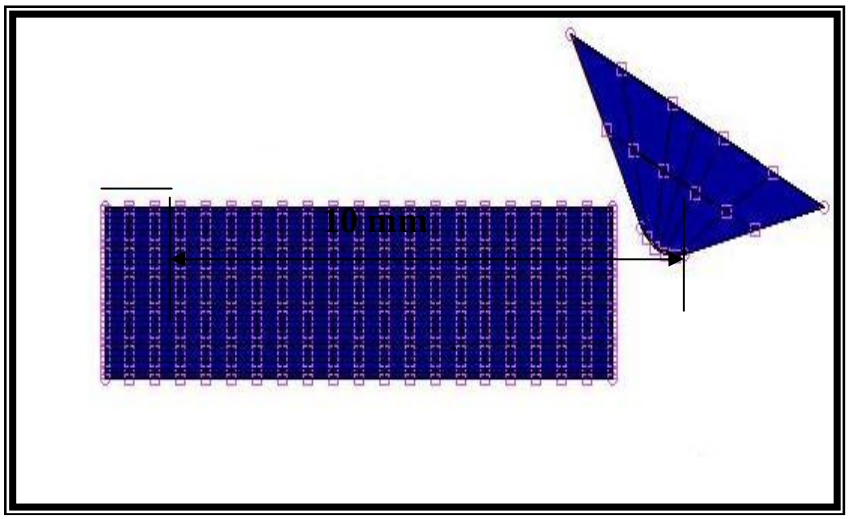

Figure (3) Representation of initial geometry and mesh for the model used in simulated tests

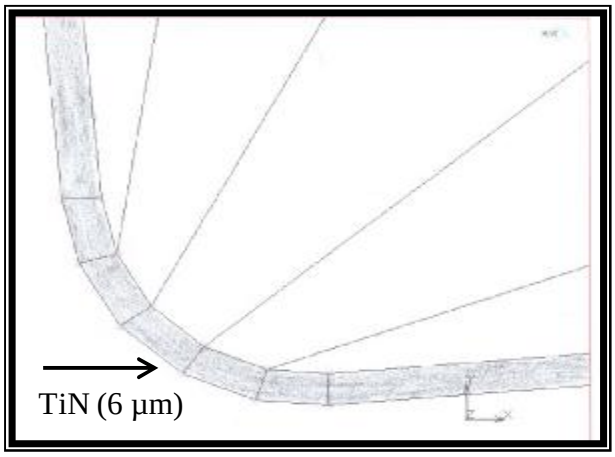

Figure (4 a) Showing tool Coated one layer TiC used in the simulation tests.

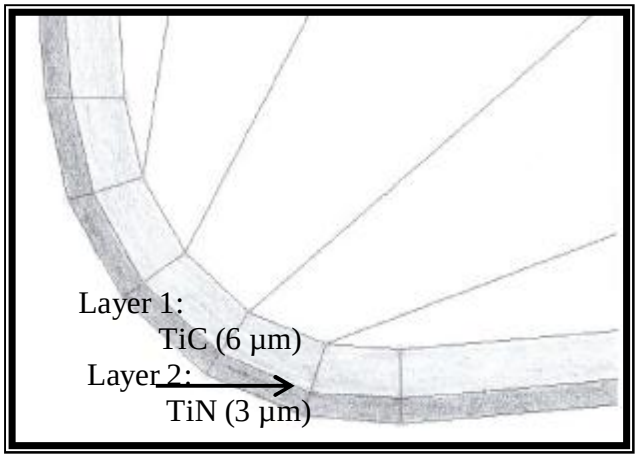

Figure (4b) A multi layer TiC/ /TiN coated tool used in the simulation tests.

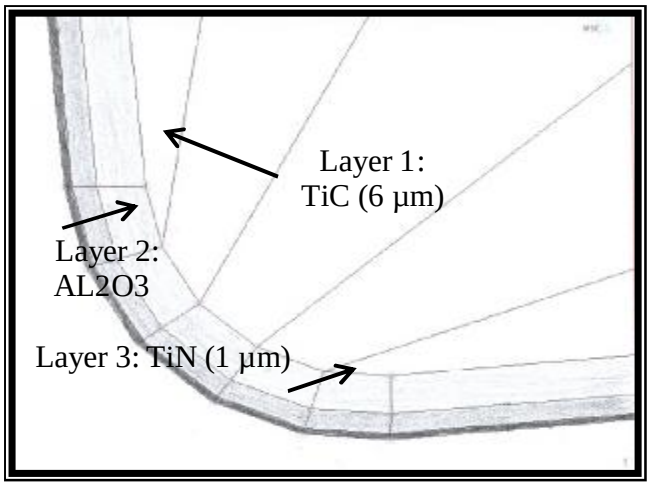

Figure (4 c) A multi layers TiC/AL_2O_3 /TiN coated tool used in the simulation tests.

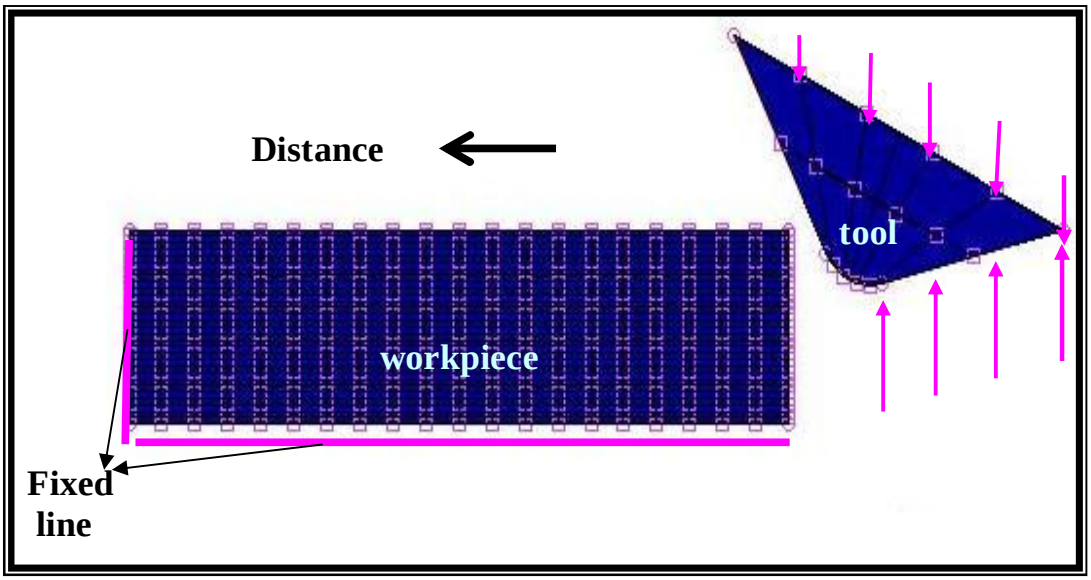

Figure (5): Representative model boundary conditions (showing the workpiece constraints, and velocity direction of the cutting tool).

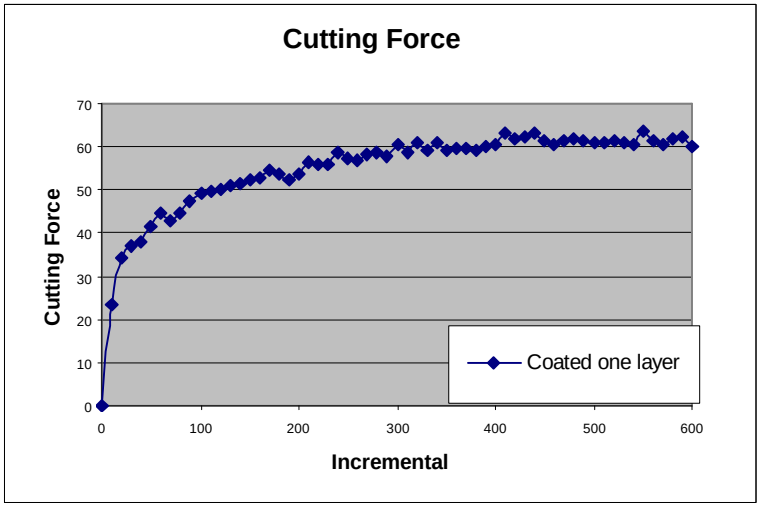

Figure (6) Cutting Forces Predicted by Finite Element Analysis in tool coated one layer.

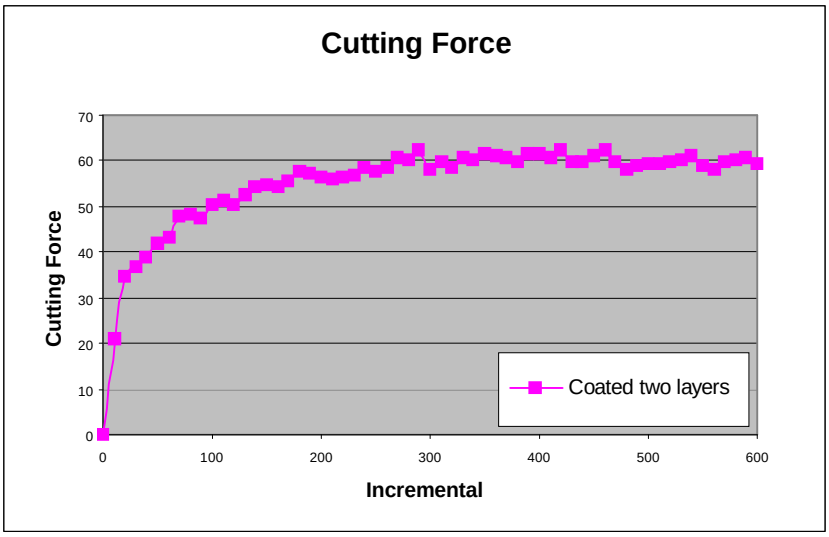

Figure (7) Cutting Forces Predicted by Finite Element Analysis in tool coated two layers.

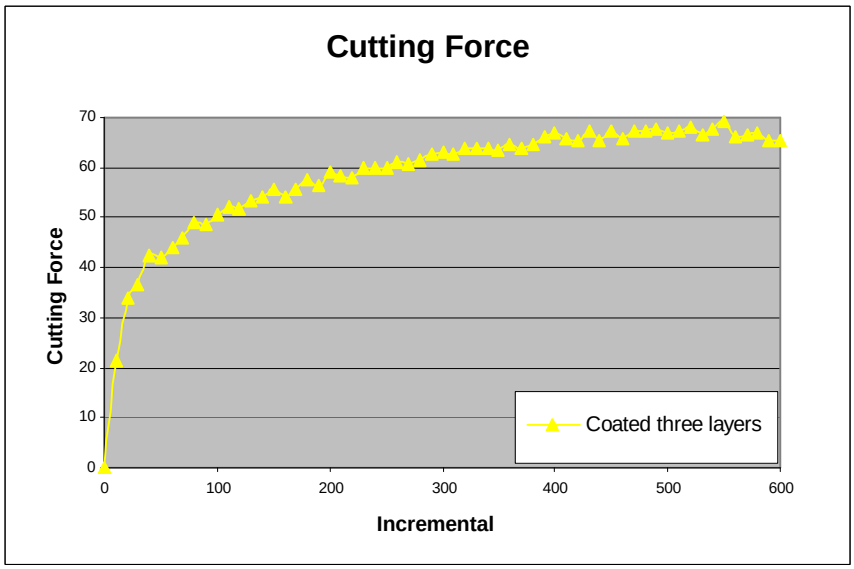

Figure (8) Cutting Forces Predicted by Finite Element Analysis in tool coated three layers.

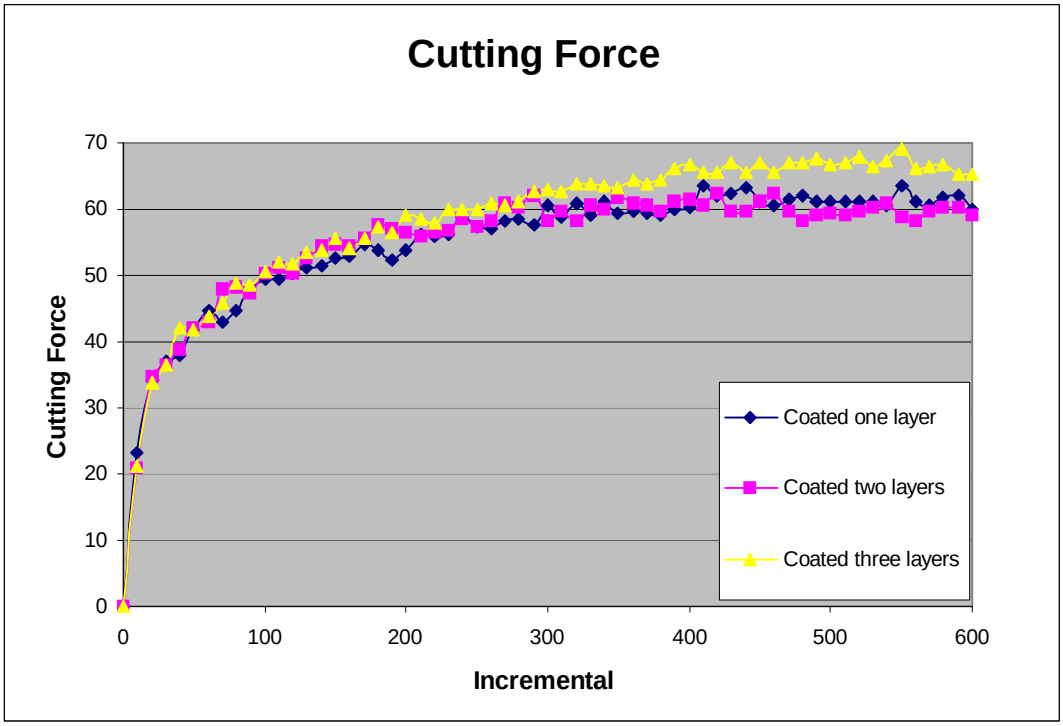

Figure (9) Cutting Forces Predicted by Finite Element Analysis in all types.

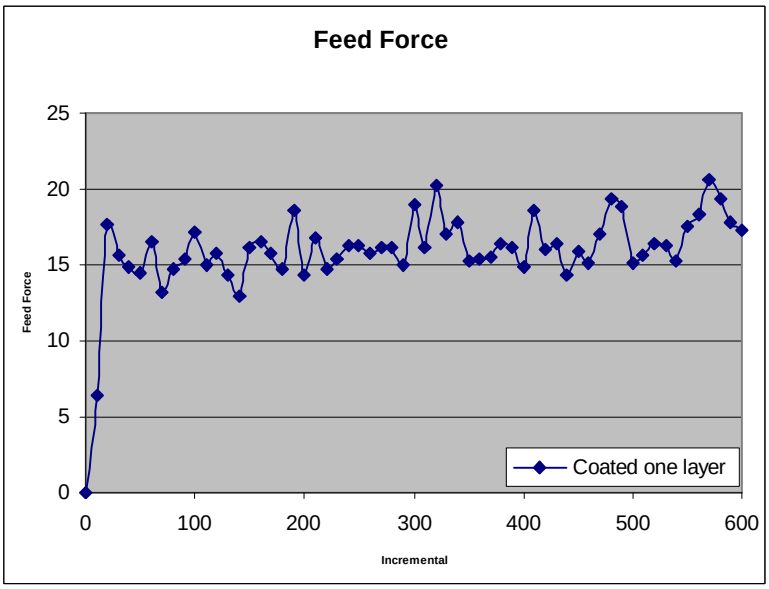

Figure (10) Feed Forces Predicted by Finite Element Analysis in tool coated one layer.

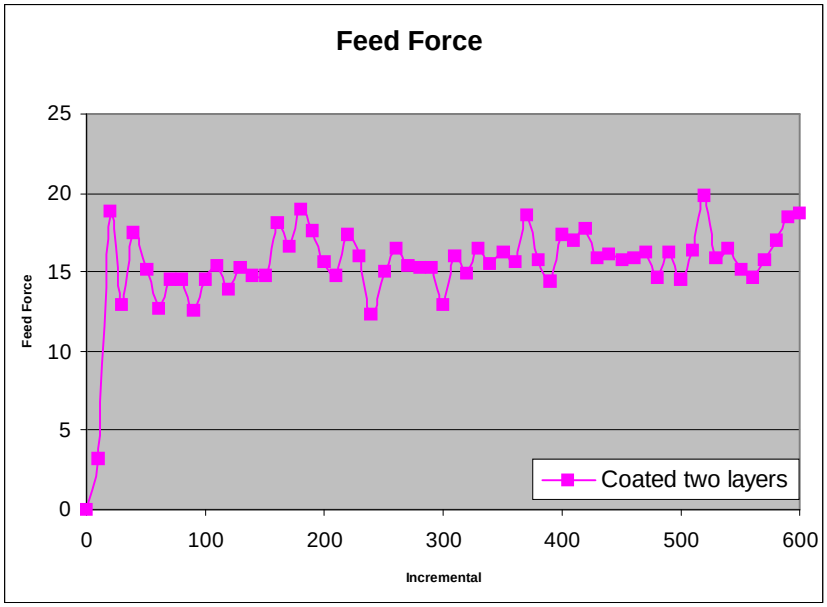

Figure (11) Feed Forces Predicted by Finite Element Analysis in tool coated two layers.

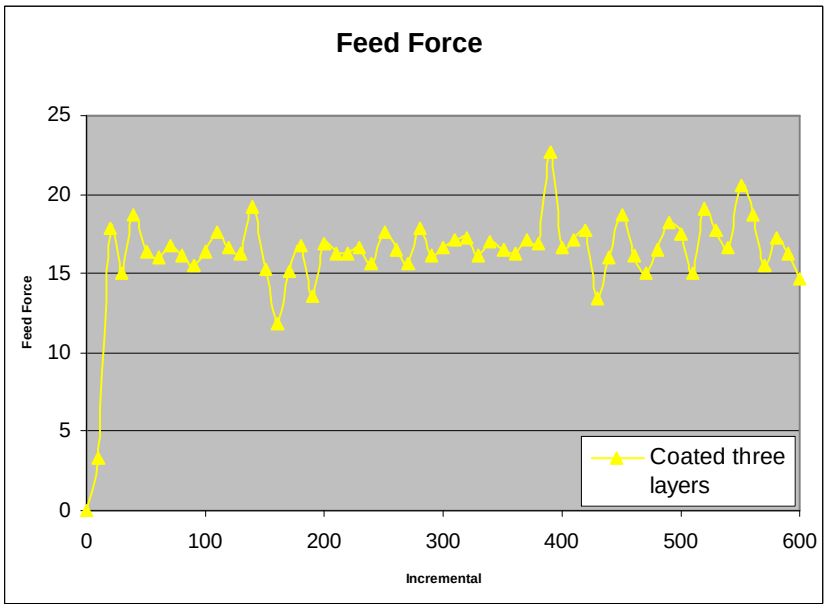

Figure (12) Feed Forces Predicted by Finite Element Analysis in tool coated three layers.

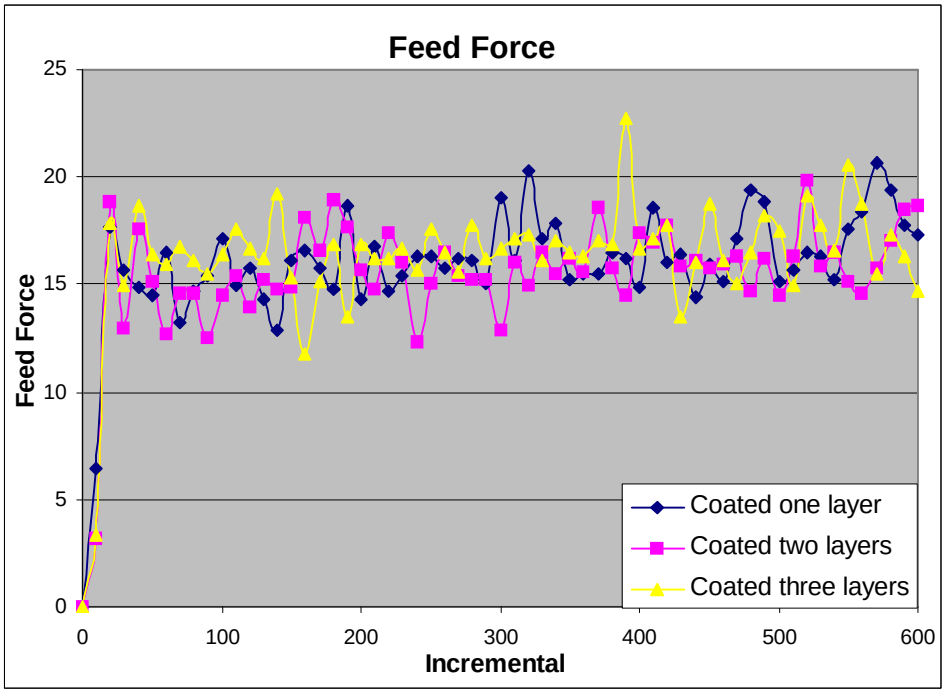

Figure (13) Feed Forces Predicted by Finite Element Analysis in all types.